PNAS

Supporting Information for

EHMT2-mediated transcriptional reprogramming drives neuroendocrine transformation in non-small cell lung cancer.

Authors: Cheng Yang[1,2], Shuxiang Ma[3], Jie Zhang[1,2], Yuchen Han[1,2], Li Wan[1,2], Wenlong Zhou[1,2], Xiaoyu Dong[1,2], Weiming Yang[1,2], Yu Chen[1,2], Lingyue Gao[1,2], Wei Cui[1], Lina Jia[1], Jingyu Yang[1], Chunfu Wu[1], Qiming Wang[3]*, Lihui Wang[1,2]*

Corresponding author: Lihui Wang[1,2], Qiming Wang[3]*

Email: lhwang@syphu.edu.cn (L.W.), qimingwang1006@126.com (Q.W.).

This PDF file includes:

Supporting Materials and Methods

Cells culture and cell viability assay

Human non-small cell lung cancer cell lines NCI-H1650, HCC4006, PC9 and HCC827 were obtained from ATCC (Gaithersburg). Cells were cultured in RPMI 1640 medium supplemented with 10% FBS (Gibco) at 37 °C in a 5% CO_2 incubator. The cell viability was determined using the MTT assay. Cells were seeded at a density of 3000 cells per well in 96-well culture plates and analyzed in a multi-mode plate reader (Molecular Devices) according to the manufacturer's instructions.

Construction process of four NE transformed cell lines and microscopic images of parental cells and SCLC transformed cells

1) Construction of erlotinib-resistant cells. The IC_{50} of erlotinib by parental cells is taken as the initial concentration. Drugs continue to treat parent cells to derive resistant cells. When the proliferation resumed, the drug concentration gradually increased by 20%. Change the culture medium and add fresh medicine once a day. Under the condition of drug resistance index < 3, drug-resistant cells remain as polyclonal population. **2) Drug resistance index.** After erlotinib induced cells continuously for one year, the polyclonal cell population with stable drug resistance index > 4 was selected for monoclonal screening by limiting dilution method. **3) Single clone cell screening.** To ensure that the obtained cells are monoclonal, the concentration of cell suspension is adjusted by using culture medium. The cell concentration is 50 ~ 60 cells /mL and 0.1 ml (5 ~ 6 cells/well) is added to each well in a 96-well culture plate to inoculate 2 rows. Add the same volume of culture solution to the remaining cell suspension for dilution, then inoculate 2 rows, and so on until the cell concentration in the culture solution added to each well is half or one cell. **4) Cell morphological screening.** Culture was continued for 7-14 days, during which observation was kept under microscope. According to NCCN standard tries to select monoclonal cell groups with SCLC characteristics to continue culture (unclear cell boundary, high nuclear-to-cytoplasmic ratio, granular chromatin and high mitotic counts, etc). **5) Other erlotinib resistance mechanisms screening.** The selected monoclonal cell population was expanded (2 ~ 4 T- clones or less were isolated from each 96-well plate) and other erlotinib resistance mechanisms such as *EGFR* T790M

mutation, *MET* or *HER2* amplification, *PIK3CA* mutation, *BRAF* mutation and *KRAS* mutation were excluded. **6) Screening of chemosensitivity.** To screen cells that are more sensitive to chemotherapy, such as SN-38 (Irinotecan active product) and Etoposide, than their parentals. **7) NE biomarkers screening.** The cells were screened again by classical SCLC markers (RB, CHGA) and new markers (EGFR, YAP). **8) CDX model confirmation.** The cells screened by the above conditions were injected into nude mice, and the pathological morphology, biomarker expression and chemosensitivity were confirmed by CDX model. Cells that accord with all the above screening conditions will be considered as NE transformed cells with SCLC characteristics (Figure S1).

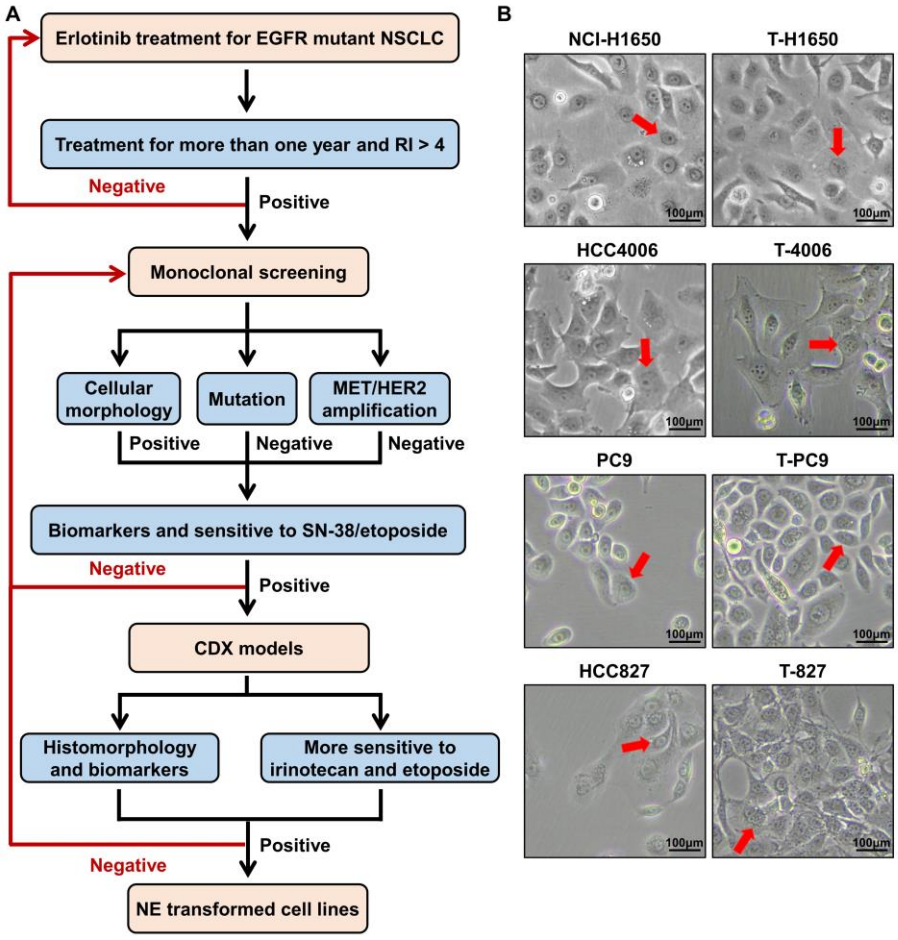

Figure S1: Construction process of four NE transformed cell lines and microscopic images of parental cells and SCLC transformed cells. *A*: The manuscript constructs drug-resistant cells through long-term induction of erlotinib. Monoclonal cell population with NE transformation

characteristics was obtained by detecting cell morphology, drug resistance mechanism, chemosensitivity and biomarkers. ***B*****:** Microscopic images of parental cells (clear nucleoli) and SCLC transformed cells (unclear cell boundary, high nuclear-to-cytoplasmic ratio, granular chromatin and high mitotic counts, etc).

Human specimens

With the formal written consent of patients, samples were collected through puncture and biopsy. Before conducted, this study was approved by the ethics committee of Affiliated Cancer Hospital of Zhengzhou University & Henan Cancer Hospital (Ethical number: 2023-331-002). All protocols adhered to the principles outlined in the Declaration of Helsinki. Formalin-fixed, paraffin-embedded (FFPE) samples were collected at the Affiliated Cancer Hospital of Zhengzhou University & Henan Cancer Hospital, China. The expression of EHMT2, YAP, CHGA and SFRP1 in samples was detected by immunohistochemistry (IHC) method.

Colony formation assay

Cells were seeded at a density of 300-500 cells per well in 12-well culture plates and the culture medium was replaced every 2 days. After culturing for 14 days, the cells were fixed with 4% paraformaldehyde for 15 min and stained with 0.1% crystal violet for 30 min. The colonies were imaged and counted.

RNA extraction and quantitative real‑time PCR

Total RNA was extracted using Trizol (Thermo Fisher Scientific) and reverse transcribed using a kit (Thermo Fisher Scientific, USA Fisher Scientific) according to the manufacturer's instructions. Quantitative RT-PCR analyses were performed in technical triplicates using a SYBR Green Supermix kit (Thermo Fisher Scientific). The following primers were used for the experiment: glyceraldehyde-3-phosphate dehydrogenase (GAPDH): reverse: 5’-CCCTCAACGACCACTTTGTCA-3’ and forward: 5’-TTCCTCTTGTGCTCTTGCTGG-3’; SFRP1: reverse: 5’- ATGTTTTGGCTTTCCACACC -3’ and forward: 5’- GTTGGAGCTGTTTGCTGTGA -3’. See Table S2 for other primers.

Transfection and lentiviral transduction

HEK293T cells were seeded in 100-mm dishes using the appropriate cell density. The plasmid siRNA or shRNA (Table S2) was introduced into the cells using lipofectamine 3000 according to the Thermo Fisher Scientific protocol. The virus-containing medium was collected by centrifugation at 3,000 rpm for 30 min to remove 293T cells after 60 hours of transfection and purified using 0.45-μm filter membranes. The purified culture medium (containing the virus) was added to the target cells in a 6-well plate. 48 hours after infection, the cells were screened with puromycin or blasticidin and tested by Western blotting and real-time PCR. Constructs for overexpression of EHMT2 and its catalytically dead mutant H1113K (pLenti-CMV-GFP-BSD) were purchased from Sito Bio-Technology. The SFRP1 overexpression constructs (pcSLenti-EF1-EGFP-F2A-Puro-CMV) were purchased from OBiO Technology.

Western blotting

Cell lysates were extracted in RIPA buffer (Cell Signaling Technology). Total histones were prepared using a Histone Extraction kit (Epigentek). Protein separation was performed using electrophoresis in 8–15% arc-bis gels. After one hour of milk blocking, the PVDF (Millipore) membrane and primary antibody (per instruction manual) were incubated overnight at 4 °C in primary antibody dilution buffer with occasional gentle shaking. Anti-rabbit IgG or anti-mouse IgG was diluted with blocking buffer for protein detection. The membrane was incubated with the diluent and the protein signal was detected after incubation with gentle shaking at room temperature for 1 hour. Primary antibodies used in this study were EHMT2 (CST, #68851), EGFR (Santa Cruz, sc-373746), RB (CST, #9309), YAP (CST, #14074), p-YAP (CST, #13008), H3K9me2 (CST, #4658), Histone3 (CST, #4499), β-catenin (CST, #8480), p70S6K (CST, #2708), p-p70S6K (CST, #9234), SMAD2 (CST, #5339), p-SMAD2 (CST, #18338), SMAD3 (CST, #9523), p-SMAD3 (CST, #9520), SFRP1 (CST, #3534), β-actin (Santa Cruz, sc-47778), CHGA (Abcam, 254557). The secondary antibody was from Cell Signaling Technology. The membrane was exposed to ECL detection reagent (Perkin Elmer) and scanned by a chemiluminescence imaging system (AZURE).

Chromatin immunoprecipitation (ChIP)-qPCR and ChIP-seq (sequencing)

ChIP assays were performed using the Chromatin Immunoprecipitation Kit (Cell Signaling Technology) according to the manufacturer's protocol. In summary, high-quality DNA was obtained

by crosslinking and chromatin fragmentation. Then, DNA bound to the target protein was obtained by immunoprecipitation and DNA purification. Immunoprecipitated DNA was analyzed by quantitative PCR (ChIP-qPCR) and next-generation sequencing technology (ChIP-seq).

Gene microarray analysis

RNA was acquired in strict accordance with official Thermo Fisher standards. The fragmented labeled RNA sample was added into a chip of a corresponding model, and chip hybridization was performed at a specific temperature and a specific rotation speed. After reaching the specified time, the gene chip elution workstation (GeneChip Fluidics Station 450) was used for washing and staining according to the corresponding protocol, and the scanner was used for scanning after completion. The scanner obtains the signal value of each probe by capturing the fluorescence signal, and the signal was converted by GCOS software.

Whole exon sequencing (WES)

Quick-frozen cell samples in liquid nitrogen were placed in dry ice and mailed to relevant places. The extracted DNA was analyzed by agarose gel electrophoresis. Qualified samples for the next experiment. Using Agilent V6 to capture and enrich human exon DNA. DNBSEQ platform for sequencing. GRCh38 was used as the reference genome for comparison.

Immunofluorescence staining

Cells were seeded into 24-well plates containing slides. After incubation for 24 h in culture solution, the samples were treated with or without drugs. Following washes, the cells were fixed with 4% paraformaldehyde. The cells were then treated with 0.5% Triton X‐100 treatment and blocked in 5% skim milk overnight at 4°C. The cells were incubated with rabbit anti‐β‐catenin polyclonal IgG. After washing, the cells were incubated with anti‐rabbit IgG (H+L), F(ab') 2 Fragment (Alexa Flour® 488 conjugate) (CST, #4412), washed, and covered in mounting medium containing DAPI. The samples were visualized with a Nikon inverted microscope.

Hematoxylin/eosin (HE) staining and immunohistochemical (IHC) staining assays

For HE staining and IHC analysis, tumor samples were embedded in paraffin and cut into sections of appropriate thickness. For HE staining, the tissue sections were stained with hematoxylin and eosin in sequence. For IHC, tissue sections were incubated with primary and secondary antibodies

of interest following antigen repair and PBS washing. After reaction with DAB reagent, the sections were viewed under the microscope (ZSGB, PV-9000). Tissue samples were detected by IHC. The percentage of positive staining was graded as follows: 0 (< 5%), 1 (5–25%), 2 (26–50%), 3 (51–75%), and 4 (>75%). The staining intensity was scored as follows: 0, no staining; 1, weak staining; 2, moderate staining; and 3, strong staining. The two scores were added together.

Cell-derived xenograft assays

For in vivo xenograft assays, 3-5×10^6 cells suspended in 100 μl of PBS were injected into the right flank of five to eight-week-old male nude mice. The subcutaneous tumor size was measured with a vernier caliper for two days and tumor volumes were calculated with the formula volume = length × width^2 × 0.5. When the tumor volume reached 60-90 mm^3, the mice were randomized into different groups. At the end of the experiment or when the subcutaneous tumor volume reached 1500 mm3, the mice were euthanized. The tumor was then removed, photographed, weighed and further analyzed. The mice were housed in SPF-grade animal rooms. To ensure the welfare of the mice, all procedures were conducted according to the guidelines of the Animal Experimental Ethics Committee of Shenyang Pharmaceutical University.

MS-PCR

DNA was extracted by kit (TIANGEN, DP304) and treated with bisulfite according to instructions (EPIGENTEK, P-1001). The primers for methylation-specific PCR (MS-PCR) of the *RB* promoter were designed as follows: forward primer 5-GGGAGTTTCGCGGACGTGAC-3 and reverse primer 5-ACGTCGAAACACGCCCCG-3. The primers for MS-PCR of the *TP53* promoter were designed as follows: forward primer 5-CTATCTTATCTATCTTCTCTATCTTC-3 and reverse primer 5-CTATCTTATCTTCTCTCATCTCTAC-3. The PCR conditions are set according to the instructions (EPIGENTEK, P-1028).

5hmC dot blot assay

DNA was extracted by kit (TIANGEN, DP304). The concentration of DNA was detected by NanoDrop 2000 and diluted to 50-200ng/μL with TE buffer. The DNA was denatured by heating to 95 °C for 10min and taking an ice bath for 5min. DNA was loaded onto a Hybond-N+ membrane (Solarbio, YA1760) and crosslinked by UV light at 245 nm for 1500J/5min. After blocking with 5 %

nonfat milk for 2 h, the membrane was incubated with 5hmC antibody (EPIGENTEK, A-1018) at 4 °C overnight. Then, the membrane was rinsed by PBST and incubated with goat anti-rabbit IgG (Thermo, 31460, 1:9000) at room temperature for 30 min. Hyperfilm ECL (PerkinElmer, NEL105001EA) was used to obtain images. The same concentration of DNA was stained by methylene blue (Solarbio, G1300) for 2 h as the control.

Flow cytometry and cell cycle detection

Select cells in good condition for the experiment. After adjusting to the same number of cells, the cells are treated according to the instructions of the kit (Solarbio, CA1510). Select the number of cells as the termination event to ensure that the number of cells detected in each group is consistent. The analysis of flow cytometry results follows the following principles: (1) The Coefficient of Variation (CV) value at 5%-10%. (2) The Root Mean Square (RMS) value is as small as possible.

Statistical analysis

All data in this article are derived from mean ± SEM of at least three independent experiments with biological replication. SPSS software was used for analysis and GraphPad Prism software was used for image rendering. The error bars may not be observable because they are covered by image symbols. The data were analyzed using Student's t-test (independent-sample t-test) and one-way analysis of variance (ANOVA) followed by Dunnett's or Tukey's multiple comparisons test. $*P < 0.05$, $**P < 0.01$, $***P < 0.001$

Supplementary Figures

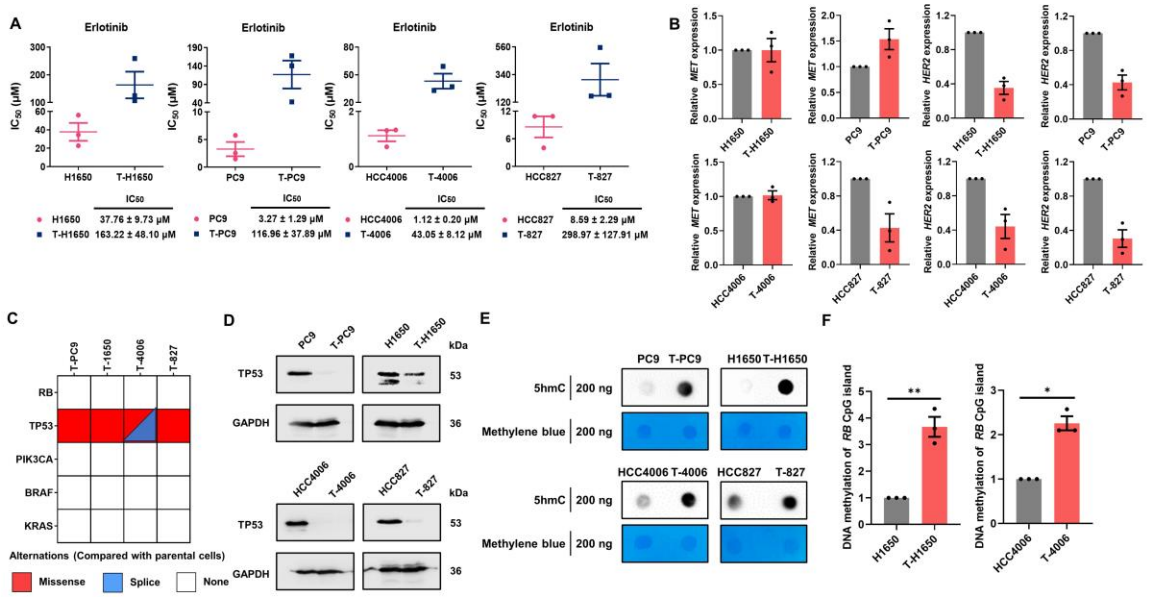

Figure S2: Establishment of transformed cell models and confirmation of potential novel biomarkers of NE transformation. *A*: IC_{50} values for parental and NE transformed cells treated with erlotinib for 48 h. Data are graphed as means ± SEM (n = 3). ***B*:** mRNA expression levels of *MET* and *HER2* were determined by qPCR in parental and NE transformed cells. ***C*:** WES detection of *RB*, *TP53*, *PIK3CA*, *BRAF* and *KRAS* mutation in four NE transformed cells, compared with the parental cell. ***D*:** Western blot was used to detect the expression of TP53 in parental cells and NE transformed cells. ***E*:** DNA methylation in the form of 5-methylcytosine (5mC) was detected by dot blot ***F*:** MS-PCR analysis of the RB promoter region in parental and NE transformed cells. *P* values were determined using Student's t-test (independent samples t-test). **P* < 0.05, ***P* < 0.01.

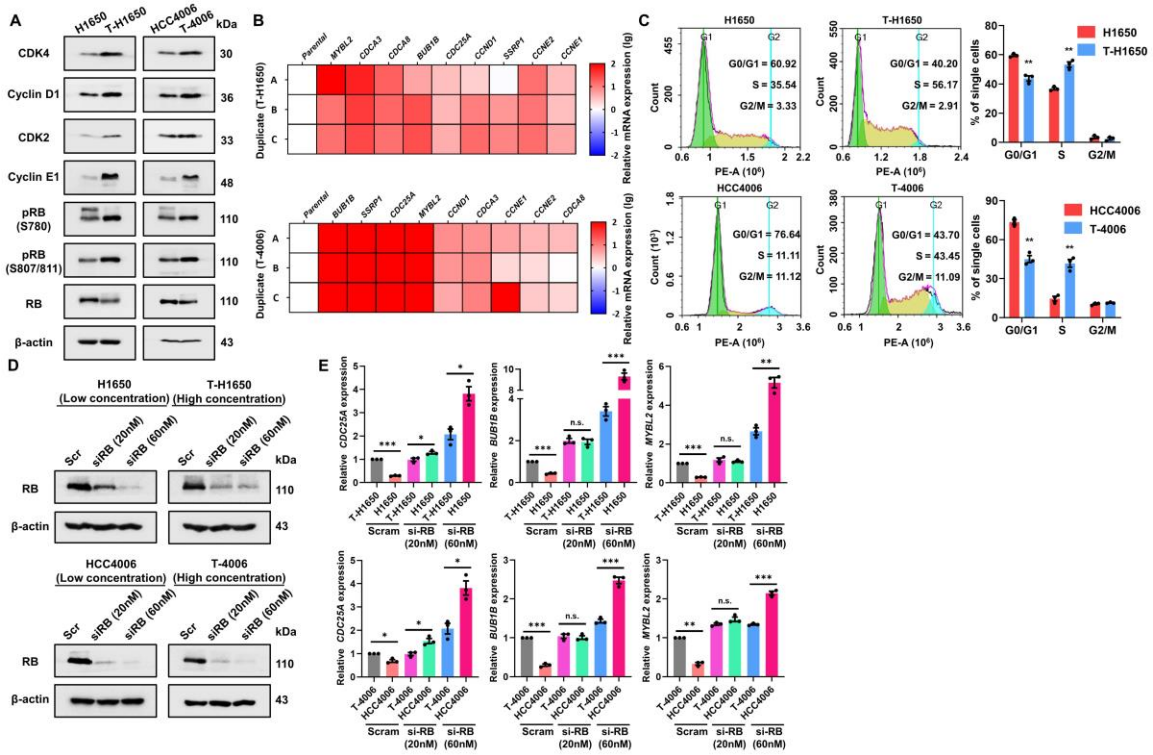

Figure S3: The status and function of RB in SCLC transformed cells. *A*: The expression of CDK4, Cyclin D1, CDK2, Cyclin E1, pRB (S780), pRB (S807/811) and RB in paired parental cells and NE-transformed cells. ***B*:** Heat map showing mRNA expression levels of target genes activated by the inactivation of RB in transformed cells compared to parental cells. Each gene is analyzed in three repeats. ***C*:** Cell cycle of parental cells and transformed cells by flow cytometry. ***D*:** Western blot analysis of RB in parental cells (Low concentration) and transformed cells (High concentration) transfected with RB siRNA or control siRNA (Scr). ***E*:** The mRNA levels of *CDC25A*, *BUB1B* and *MYBL2* were detected by qPCR in RB siRNA treated parental cells and transformed cells. *P* values were determined using Student's t-test (Independent samples t-test, n = 3). **P* < 0.05, ***P* < 0.01, ****P* < 0.001.

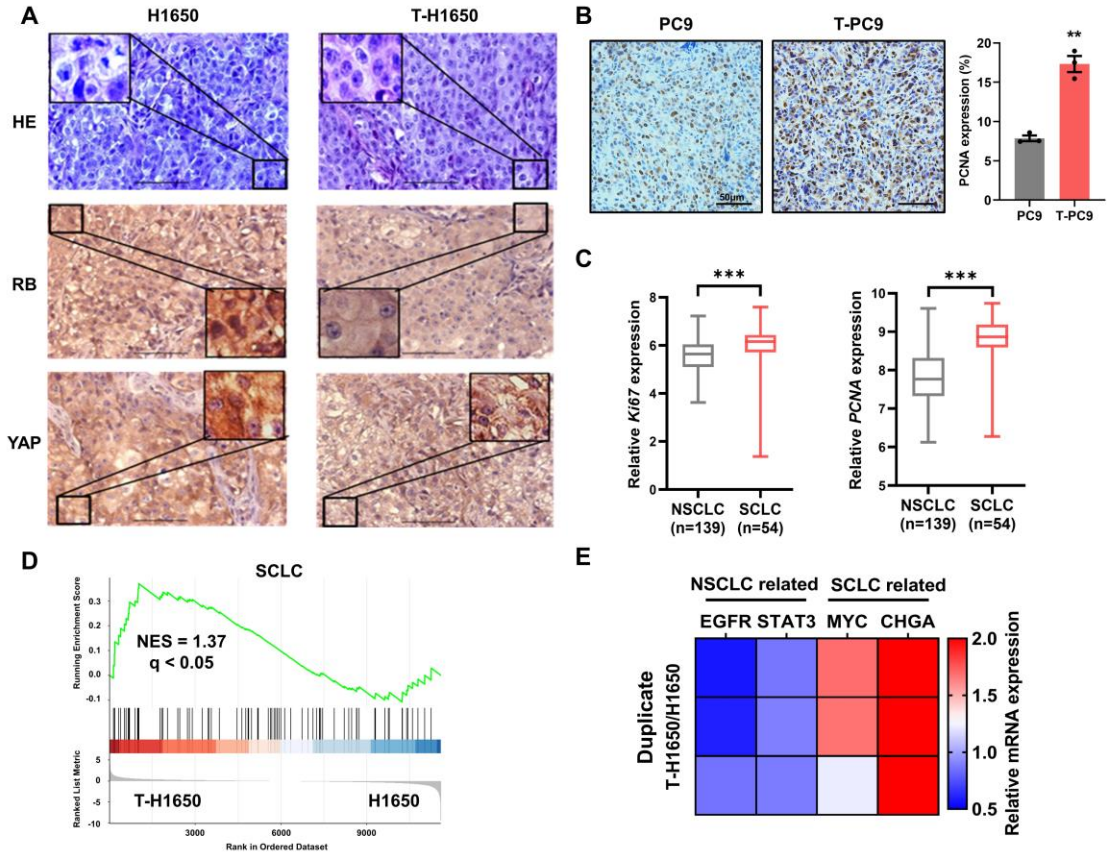

Figure S4: Histological analyses of xenograft tumors derived from transformed cell lines and RNA-seq analysis of transformed cell lines. *A*: Representative images of xenograft tumor sections subjected to HE staining and IHC staining. HE staining was performed on tumor tissue sections derived from T-H1650-CDX xenograft mice. Scale bar, 50 μm. Data are graphed as means ± SEM (n = 3). ***B*:** IHC staining of PCNA for in situ analysis of NE transformation status and cell proliferation in xenograft tumors. PCNA is a marker of cell proliferation. Scale bar, 50 μm. Data are graphed as means ± SEM (n = 3). ***P* < 0.01, two-tailed Student's t test. ***C*:** Ki67 and PCNA mRNA expression levels in NSCLC (n = 139) and SCLC (n = 54). Data are from the CCLE 23Q4 Public. ****P* < 0.001, two-tailed Student's t test. ***D*:** GSEA enrichment plot of the SCLC gene set with the corresponding statistical metrics shown. The analysis was carried out on paired cell lines (T-H1650/H1650). ***E***: mRNA expression levels of *EGFR, STAT3, MYC* and *CHGA* were determined by gene microarray in H1650 and T-H1650 cells. Values for T-H1650/H1650 are presented as heat maps.

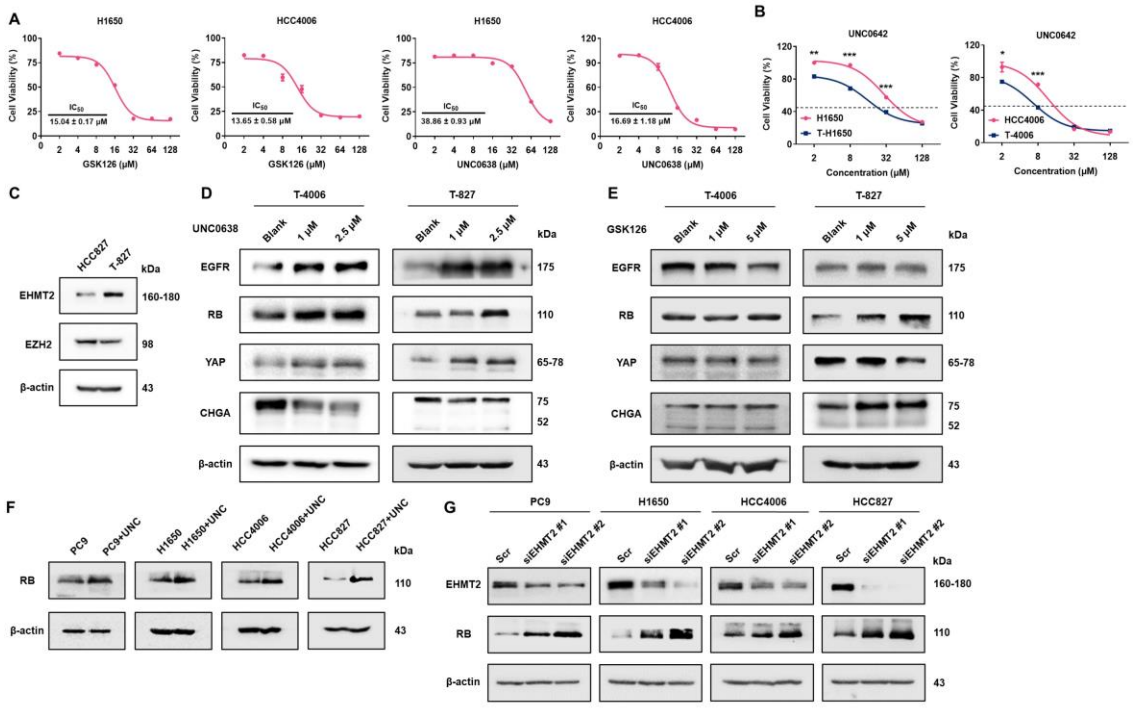

Figure S5: Acquired resistance to EGFR TKIs in NE-transformed cells is associated with EHMT2. *A*: MTT assay was used to detect the sensitivity of *EGFR* mutant parental cells after exposure to GSK126 and UNC0638 for 48 h. Data are graphed as means ± SEM (n = 3). ***B*:** Sensitivity of NE-transformed cells compared to parental cells to inhibitors at four concentrations. H1650, HCC4006, T-H1650 and T-4006 cells were treated with UNC0642. Data are graphed as means ± SEM (n = 3). **P* < 0.05, ***P* < 0.01, ****P* < 0.001, two-tailed Student's t test. ***C*:** Protein abundance of EHMT2 and EZH2 in paired parental cells and NE-transformed cells (827/T-827). ***D* and *E*:** Effect of UNC0638 ***D*:** or GSK126 ***E*:** on the abundance of NE transformation biomarkers in NE transformed cells. Cells were exposed to inhibitors for 48 h. ***F*:** The expression of RB in four NSCLC cells treated with EHMT2 inhibitor UNC0638 (2.5μM). ***G*:** The expression of EHMT2 and RB in four NSCLC cells treated with EHMT2 siRNA (50nM).

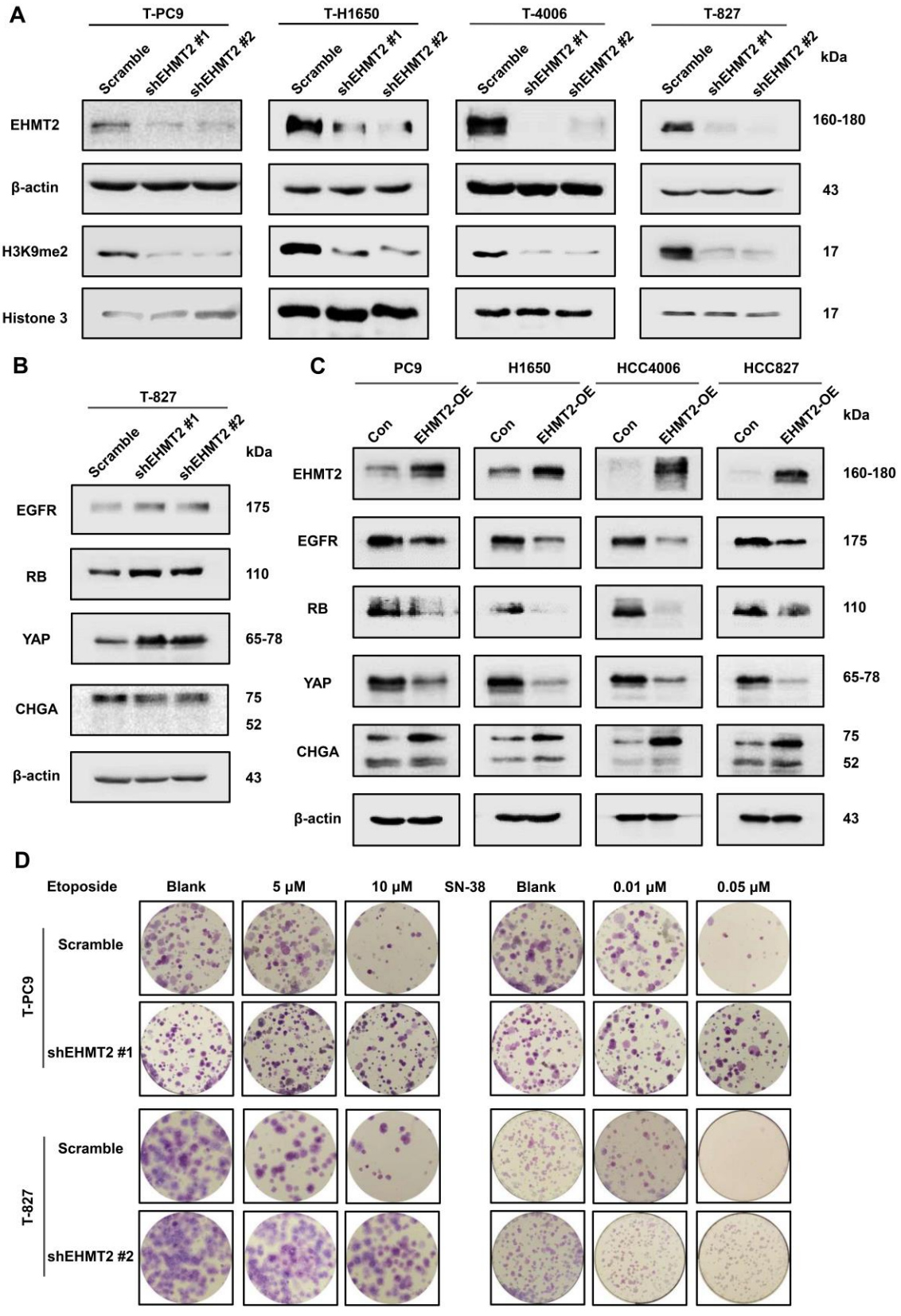
A
T-PC9
T-H1650
T-4006
T-827
Scramble
shEHMT2 #1
shEHMT2 #2
kDa
EHMT2
160-180
β-actin
43
H3K9me2
17
Histone 3
17
B
T-827
Scramble
shEHMT2 #1
shEHMT2 #2
kDa
EGFR
175
RB
110
YAP
65-78
CHGA
75
52
β-actin
43
C
PC9
H1650
HCC4006
HCC827
Con
EHMT2-OE
kDa
EHMT2
160-180
EGFR
175
RB
110
YAP
65-78
CHGA
75
52
β-actin
43
D
Etoposide
Blank
5 μM
10 μM
SN-38
Blank
0.01 μM
0.05 μM
T-PC9
Scramble
shEHMT2 #1
T-827
Scramble
shEHMT2 #2

Figure S6: Increased expression of catalytically active EHMT2 contributes to the EGFR TKI resistance in NE transformation. *A*: Effect of lentiviral *EHMT2* knockdown on the abundance of EHMT2 and H3K9me2 in NE-transformed cells. ***B*:** Effect of *EHMT2* knockdown on the protein abundance of NE transformation biomarkers in T-827 cells. ***C*:** The expression of EHMT2 and biomarkers in EHMT2 overexpression NSCLC cells and control cells. ***D*:** Colony formation assay showing the effect of *EHMT2* knockdown on the sensitivity of T-PC9 and T-827 cells to etoposide and SN-38. The cells were treated with etoposide (5 μM and 10 μM) and SN-38 (0.01 μM and 0.05 μM) for 2 weeks for colony formation analysis.

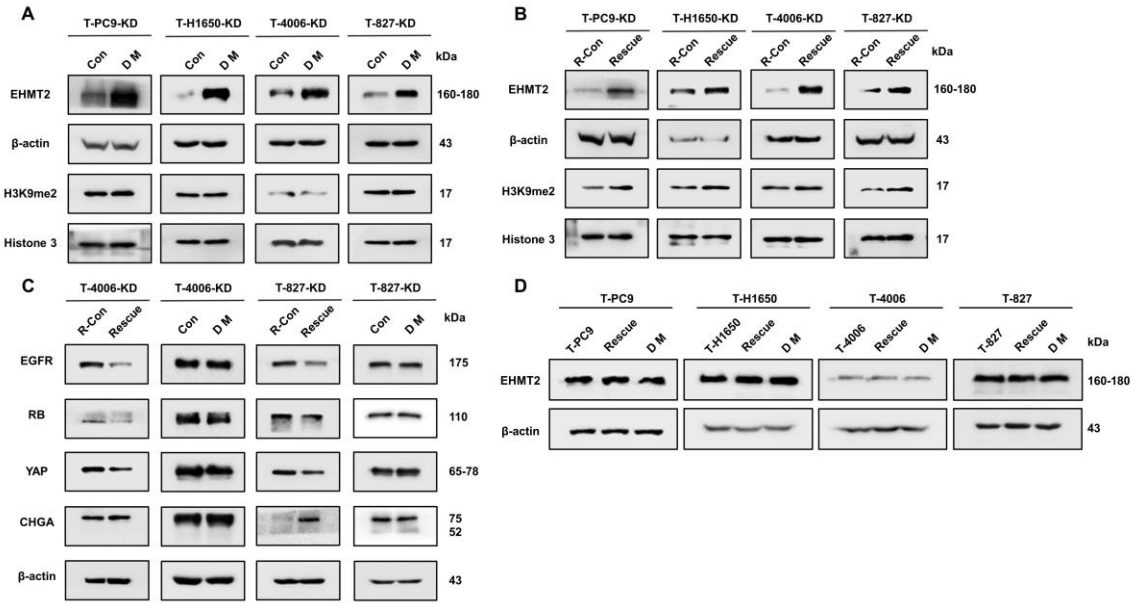

Figure S7: In NE-transformed cells, EGFR TKI resistance involves increased EHMT2 expression and depends on EHMT2-catalyzed methylation. *A*: Effect of the *EHMT2* dead mutant on EHMT2 and H3K9me2 abundance in *EHMT2* knockdown NE-transformed cells. ***B*:** Effect of *EHMT2* rescue on EHMT2 and H3K9me2 abundance in *EHMT2* knockdown NE-transformed cells. ***C*:** The protein abundance of NE transformation biomarkers was detected by western blot in rescue cells (expressing WT EHMT2) and DM cells (expressing the catalytic dead mutant of EHMT2) in EHMT2 knockdown NE-transformed cell lines. ***D*:** Abundance of EHMT2 protein in rescue cells and DM cells compared to parental cells.

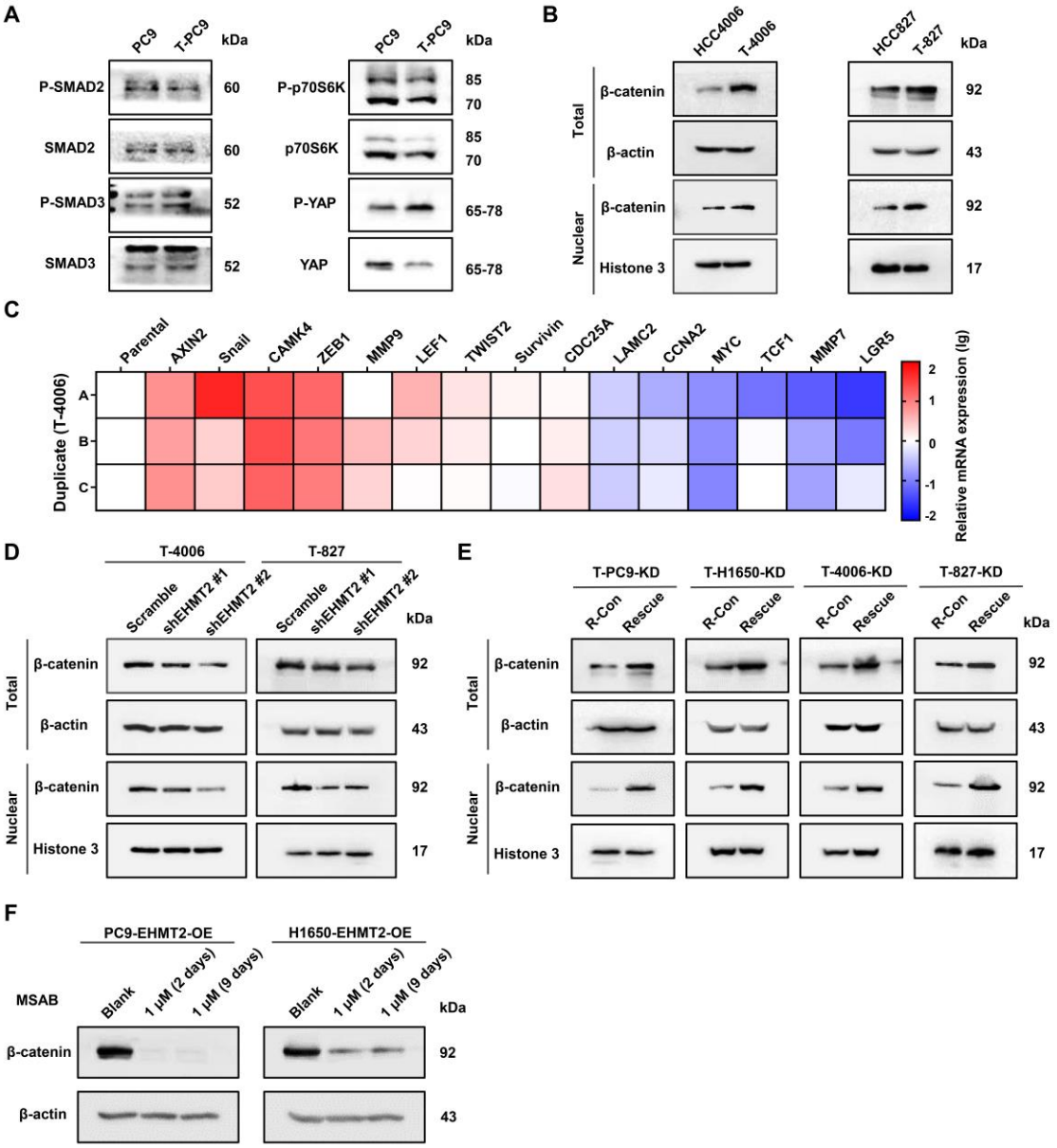

Figure S8: EHMT2 activates the WNT/β-catenin pathway in NE transformation. ***A*****:** The abundance of key proteins in the mTOR, TGF-β and Hippo pathways was detected by Western blot in parental cells and NE-transformed cells. ***B*****:** The abundance of β-catenin protein was detected by Western blot in parental cells and NE-transformed cells. ***C*****:** Heat map showing mRNA expression levels of downstream genes activated by the WNT/β-catenin pathway in T-4006 cells compared to parental HCC4006 cells. Analysis of each gene is repeated three times. ***D*****:** Western blot showing the effect of *EHMT2* knockdown on the abundance of β-catenin protein in NE-transformed cells. ***E*****:** Western blot showing the effect of *EHMT2* rescue on the abundance of β-

catenin protein in NE-transformed cells. ***F*:** Inhibitory effect of WNT/β-catenin pathway inhibitor in short-term and long-term treatment.

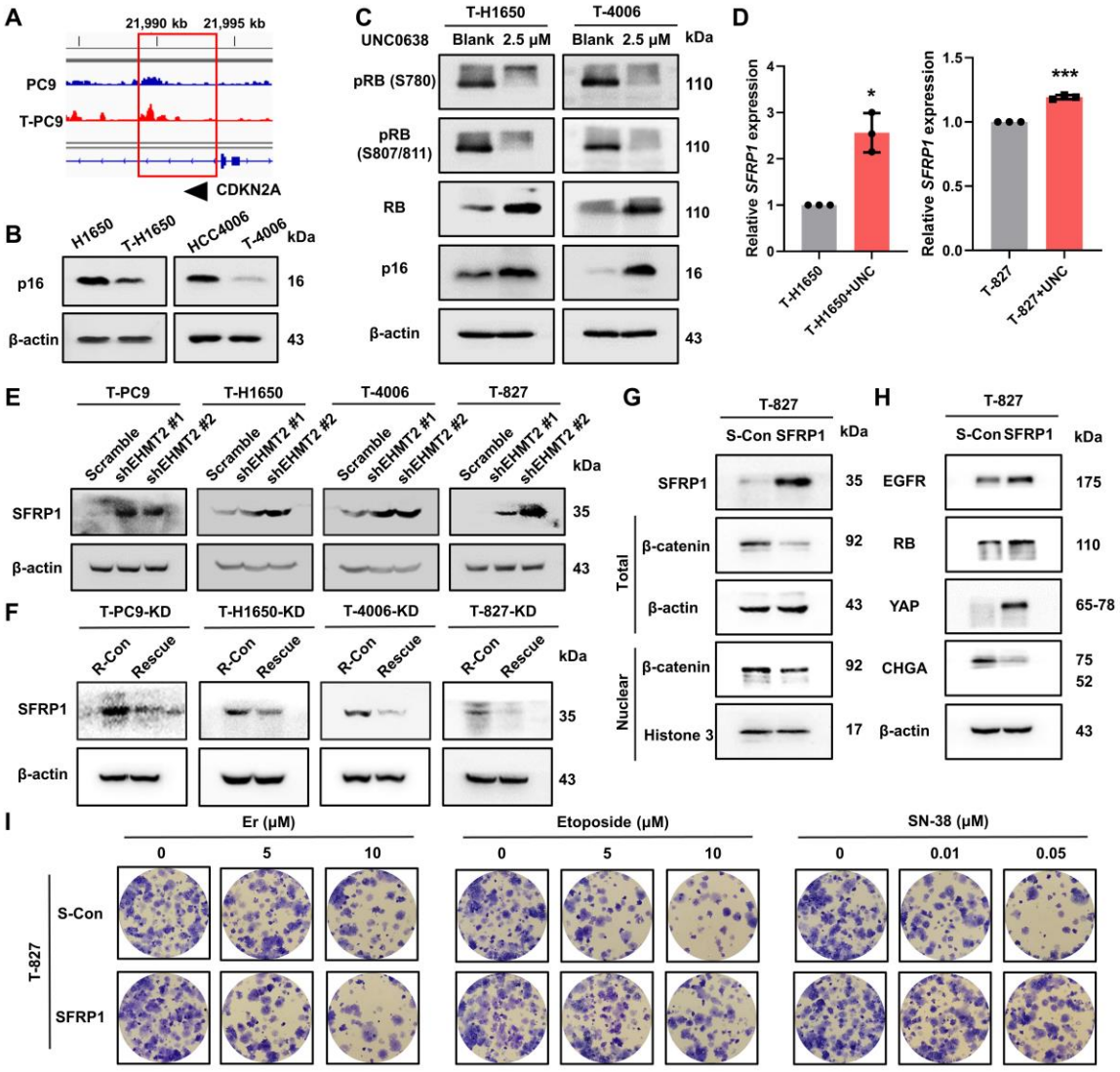

Figure S9: Mechanism of RB phosphorylation and EHMT2 up-regulates the WNT/β-catenin pathway by repressing SFRP1 to boost NE transformation and erlotinib resistance. *A*: H3K9me2 ChIP-seq reads in PC9 and T-PC9 cells. The *CDKN2A* promoter regions are enclosed in the red rectangle. ***B*:** The expression of p16 in paired parental cells and NE-transformed cells. ***C*:** The expression of pRB (S780), pRB (S807/811), RB and p16 in NE-transformed cells and UNC0638 treatment cells (2.5 μM, 48 h). ***D*:** *SFRP1* mRNA expression in UNC0638 treatment NE-transformed cells was assayed by RT-qPCR analysis compared with NE-transformed cells (2.5 μM, 48 h). ***E*:** The abundance of SFRP1 protein in *EHMT2* knockdown NE-transformed cells. ***F*:** The abundance of SFRP1 protein in *EHMT2* rescue NE-transformed cells. ***G*:** Western blots confirming the overexpression of SFRP1, and demonstrating the effect of SFRP1 overexpression on the

abundance of β-catenin protein in T-827 cells. ***H*:** Western blots showing the effect of SFRP1 overexpression on the abundance of NE transformation biomarker proteins in T-827 cells. ***I*:** Colony formation assays showing the effect of SFRP1 overexpression on erlotinib, etoposide and SN-38 sensitivity in T-827 cells. The cells were treated with erlotinib (5 μM and 10 μM), etoposide (5 μM and 10 μM) and SN-38 (0.01 μM and 0.05 μM) for 2 weeks for colony formation analysis.

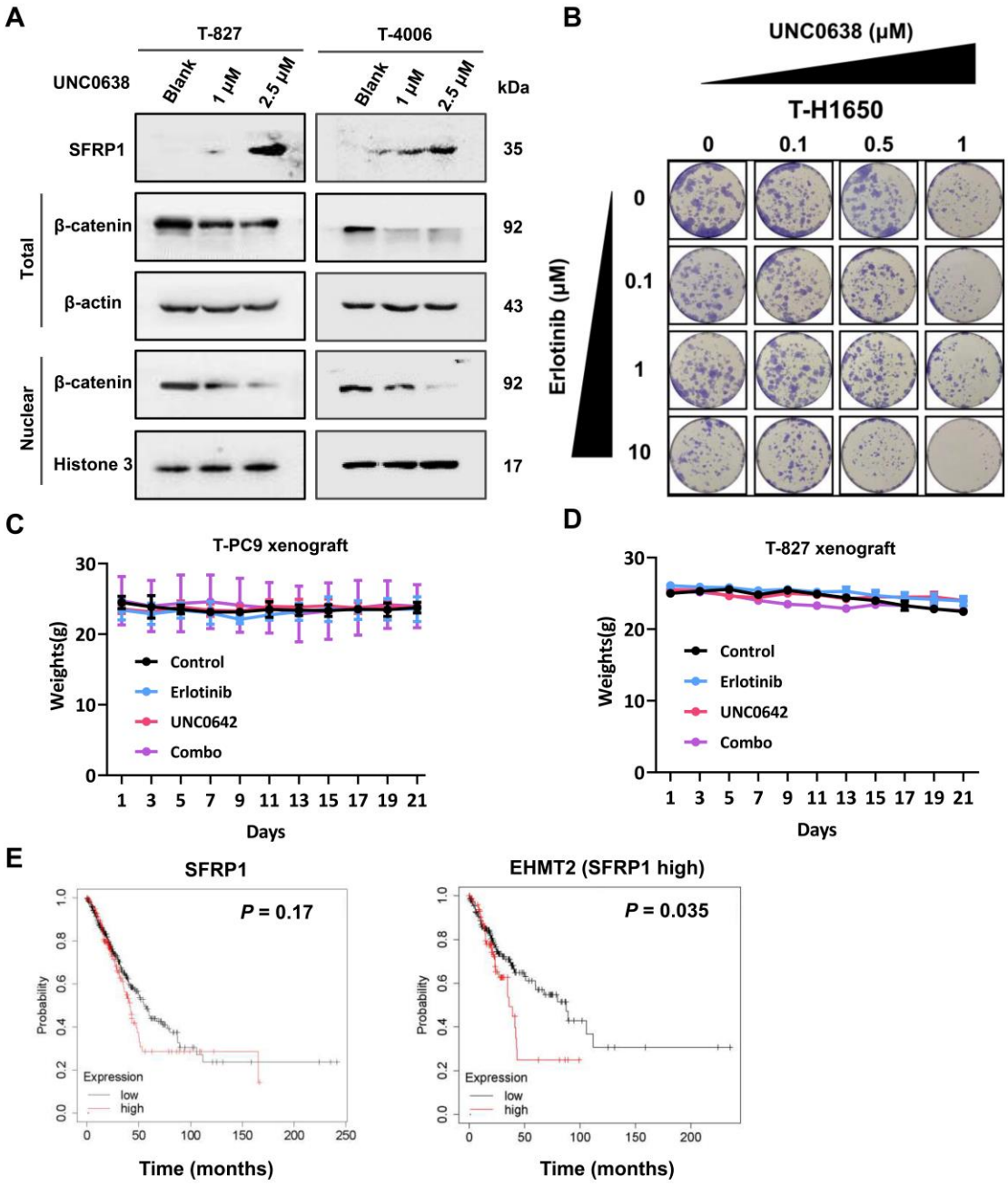

Figure S10: Therapeutic targeting of EHMT2 delays EGFR-TKI resistance in vitro and in vivo. *A*: Western blots showing the abundance of SFRP1 and β-catenin in NE-transformed cells without or with UNC0638 treatment for 48 h. ***B*:** Drug concentration matrices showing the viability of T-H1650 cells after treatment with gradient doses of UNC0638 and erlotinib for 2 weeks. ***C* and *D*:** Body weight changes in the T-PC9 xenograft mice (***C***) and the T-827 xenograft mice (***D***). ***E*:** Left: Survival status of patients with lung adenocarcinoma with high or low SFRP1 expression.

Right: Survival status of lung adenocarcinoma patients with high or low EHMT2 expression when SFRP1 expression is high. Data are from the Kaplan-Meier Plotter database.

Table S1. The 55 pathways which are enriched in transformed cells

Intersection pathway	
Spliceosome	Lysine degradation
Cell cycle	Tight junction
Nucleocytoplasmic transport	Thermogenesis
Herpes simplex virus 1 infection	Biosynthesis of cofactors
Ribosome biogenesis in eukaryotes	Pathways in cancer
mRNA surveillance pathway	Human immunodeficiency virus 1 infection
Ubiquitin mediated proteolysis	Shigellosis
RNA degradation	Hepatocellular carcinoma
Amyotrophic lateral sclerosis	mTOR signaling pathway
Huntington disease	Proteoglycans in cancer
Oocyte meiosis	Bacterial invasion of epithelial cells
Ribosome	Gastric cancer
Spinocerebellar ataxia	Autophagy - animal
Parkinson disease	Signaling pathways regulating pluripotency of stem cells
Pathways of neurodegeneration - multiple diseases	Chemical carcinogenesis - reactive oxygen species
Alzheimer disease	Calcium signaling pathway
Proteasome	Epstein-Barr virus infection
Prion disease	TGF-beta signaling pathway
Viral carcinogenesis	Diabetic cardiomyopathy
Endocytosis	Glioma
Basal transcription factors	Retrograde endocannabinoid signaling
RNA polymerase	Prostate cancer
Aminoacyl-tRNA biosynthesis	Apoptosis
Human T-cell leukemia virus 1 infection	Sphingolipid signaling pathway
Hippo signaling pathway	Protein processing in endoplasmic reticulum
Wnt signaling pathway	Transcriptional misregulation in cancer
Chronic myeloid leukemia	

Table S2. Sequences of oligonucleotides and shRNAs

Target Genes	Sequence/TargetSeq
TCF1	forward: AACACCTCAACAAGGGCACTC reverse: CCCCACTTGAAACGGTTCCT
ZEB1	forward: TTACACCTTTGCATACAGAACCC reverse: TTTACGATTACACCCAGACTGC
CAMK4	forward: TCGTCCTGCTCTTCGGTCACC reverse: TCCCTGTTGGAGCCGTCGATC
MMP7	forward: GAGTGAGCTACAGTGGGAACA reverse: CTATGACGCGGGAGTTTAACAT
CDC25A	forward: TTCCTCTTTTTACACCCCAGTCA reverse: TCGGTTGTCAAGGTTTGTAGTTC
MYC	forward: GTCAAGAGGCGAACACACAAC reverse: TTGGACGGACAGGATGTATGC
Snail	forward: CCCAATCGGAAGCCTAACTACAGC reverse: AAACCTCCTGGAGCCCAGAACC
MMP9	forward: AGACCTGGGCAGATTCCAAAC reverse: CGGCAAGTCTTCCGAGTAGT
Survivin	forward: AGGACCACCGCATCTCTACAT reverse: AAGTCTGGCTCGTTCTCAGTG
LGR5	forward: CTGTCCTTGCCTGTGCTGCTG reverse: CGGGCTCGCAATGACAGTGTG
LAMC2	forward: TGCCTCTGCTTCTCGCTCCTC reverse: CCAGGGCTGAGATGTTTCCTTGTG
TWIST2	forward: GGCGCTACAGCAAGAAGTCG reverse: TGCAGCTCCTCGAAGGACTG
AXIN2	forward: TACACTCCTTATTGGGCGATCA reverse: TTGGCTACTCGTAAAGTTTTGGT
CCNA2	forward: AGCAGTGATGTTGGGCAACTCTG reverse: TGCCTTTTCCGGGTTGATATTCTCC
LEF1	forward: ACGGACGAGATGATCCCCTTCAAG reverse: TGTCAGCTAAATCGCCTTCCTCTTC
BUB1B	forward: GCACCGACAATTCCAAGCTC reverse: TGTGCTTCGTTGTGGTACAGA
SSRP1	forward: GTCTGTTTTTGTTACCCCACAA reverse: TTCTTCCTCGTTCATGTTCAGA
MYBL2	forward: CCGGAGCAGAGGGATAGCA

	reverse: CAGTGCGGTTAGGGAAGTGG
CCND1	forward: CAATGACCCCGCACGATTTC reverse: CATGGAGGGCGGATTGGAA
CDCA3	forward: TCTCCTACTCTTGGTATTGCAC reverse: TACTTCACTCAGCTGTTTCACC
CCNE1	forward: GCCAGCCTTGGGACAATAATG reverse: CTTGCACGTTGAGTTTGGGT
CCNE2	forward: TCAAGACGAAGTAGCCGTTTAC reverse: TGACATCCTGGGTAGTTTTCCTC
CDCA8	forward: CCGTGAAGTGGAAATACGAATC reverse: GGATCTCGATGTTGTAGAGGTT
EHMT2	Scr: TTCTCCGAACGTGTCACGT sh #1: GGATGCTTCTGAAGCTCAA sh #2: GGTTTGCGCTTCAACTCAA NC: UUCUCCGAACGUGUCACGUdTdT (sense (5'-3')) ACGUGACACGUUCGGAGAAdTdT (antisense (5'-3')) siEHMT2-1: GGAUGAAUCUGAGAAUCUUdTdT (sense (5'-3')) AAGAUUCUCAGAUUCAUCCdTdT (antisense (5'-3')) siEHMT2-2: GUCUGAAGUUGAAGCUCUAdTdT (sense (5'-3')) UAGAGCUUCAACUUCAGACdTdT (sense (5'-3'))
RB	NC: UUCUCCGAACGUGUCACGUdTdT (sense (5'-3')) ACGUGACACGUUCGGAGAAdTdT (antisense (5'-3')) siRB: GACCAACUGAUCACCUUGAdTdT (sense (5'-3')) UCAAGGUGAUCAGUUGGUCdTdT (antisense (5'-3'))

Table S3. Human specimens

Patient	pre-LUAD	post-SCLC-1	post-SCLC-2
1	B2003150	B2129243	B2201068
2	B1803810		
3	B1902582		
4		B1801134	
5		B1820389	
6		B2004118	
7		B2120575	

Data file S1. Raw data for main figures and supplementary figures